ELSEVIER

Journal of Alloys and Compounds 323–324 (2001) 315–320

Journal of ALLOYS AND COMPOUNDS

www.elsevier.com/locate/jallcom

Growth and 10 K spectroscopy of Nd^{3+} in $NaBi(WO_4)_2$ single crystal

A. Méndez-Blas, V. Volkov, C. Cascales*, C. Zaldo

Instituto de Ciencia de Materiales de Madrid, Consejo Superior de Investigaciones Científicas, Cantoblanco, 28049 Madrid, Spain

Abstract

The experimental procedures to grow Nd doped $NaBi(WO_4)_2$ single crystals by the Czochralski method and the difficulties or limitations encountered for doping are described. Nd concentrations in the crystal up to 0.3×10^{20} cm^{-3} have been produced with optical quality. Polarised optical absorption and photoluminescence of Nd^{3+} ion in this host have been studied at 10 K and the relative energies of 90 levels have been determined. An attempt to explain the large observed spectroscopic line-widths has been conducted through crystal field calculations of these levels supposing either a single Nd position with C_2 symmetry or two centres both with S_4 point symmetry. The latter assumption produces energy differences between both optical centres that can justify the enlargement of lines, but it is not consistent with the OA intensity changes observed in polarised spectra. The coexistence of several sites with statistically modified ordering of the short range Na and Bi cation distribution is suggested to account for this disagreement. © 2001 Elsevier Science B.V. All rights reserved.

Keywords: Phosphors; Crystal growth; Crystal field; Optical properties; Luminescence

1. Introduction

Crystals of double tungstates and molybdates with structure related to the $CaWO_4$ scheelite-type are particularly promising optical materials [1], whose spectroscopic, laser, and χ^3 non-linear optical properties, especially when doped with Nd^{3+}, have been studied [2]. Among them, sodium bismuth tungstate with stoichiometry $NaBi(WO_4)_2$ (NBW) presents several interesting features, mainly concerning the luminescence properties [3], and the polarised IR and Raman spectra characteristics [4,5]. The relationship between these measurements and short-range order as well as non-random distribution of Na^+ and Bi^{3+} ions in the crystal has been analysed [6].

Continuing a preliminary crystal growth study on this system [7], the current work presents new results on the growth and the spectroscopic properties of Nd^{3+} doped NBW crystals. From 10 K polarised optical absorption and photoluminescence measurements, the relative energy of 90 crystal field levels has been identified and 85 of them used to perform a single electron crystal field analysis of the Nd^{3+} centre. The symmetry of the point site occupied by Nd^{3+} when it replaces Bi^{3+} in the NBW matrix as well as the large widths of the observed spectral line profiles are discussed and an attempt to explain them is made.

2. Crystal structure

$NaBi(WO_4)_2$ is described as belonging to the tetragonal scheelite-type crystal structure. A summary of the crystal chemistry of NBW has been previously given [6]. Nevertheless, some contradictory results about the space group S.G. and the symmetry of the point sites occupied by the metallic cations arise from earlier X-ray studies by the same [5] or different [8] authors. While initially [5,8] the symmetry of the structure was proposed to correspond to the centrosymmetric S.G. $I4_1/a$ (No. 88), $Z=2$, a more recent single-crystal X-ray analysis [6] described it in the non-centrosymmetric S.G. $I\bar{4}$ (No. 82), $Z=2$. In any case, the structure is built-up with WO_4 tetrahedral groups and NaO_8 and BiO_8 distorted square antiprisms. In the first model Na^+ and Bi^{3+} ions occupy statistically an unique position, with S_4 [8] or C_2 local site symmetry [5], however, in the non-centrosymmetric model these cations share two non-equivalent lattice sites (2*c* and 2*b* Wyckoff positions for Bi1 and Bi2, respectively) with local symme-

---

*Corresponding author. Tel.: +34-91-334-9027; fax: +34-91-372-0623.

E-mail addresses: ccascales@icmm.csic.es (C. Cascales), cezaldo@icmm.csic.es (C. Zaldo).

0925-8388/01/$ – see front matter
PII: S0925-8388(01)01099-4

try S_4 but different occupancy factors, namely 60%Bi + 40%Na and 40%Bi + 60%Na for 2*c* and 2*b* sites, respectively.

3. Crystal growth

An important step in growing $NaBi_{1-x}Nd_x(WO_4)_2$ single crystals with high optical quality is the synthesis of the correct phase before pulling. This has been achieved by a two-step process. First, the intermediate $Na_2W_4O_{13}$ phase was sintered by 100 h/760°C annealing of 99% WO_3 and 99.5% $NaCO_3$ stoichiometric mixtures. Further, the Nd doped NBW phase was obtained by reacting this intermediate phase with 99.9% Bi_2O_3 and Nd_2O_3 during 100 h at 860°C.

During sintering and crystal pulling of NBW crystals we observed evaporation and condensation on the seed-holder and crucible walls of the evaporated material. We have determined by ionic coupling plasma (ICP) spectrometry that the composition of the evaporated material is $Na_{0.5}K_{0.5}Bi(MoO_4)_2$. The presence of Mo is likely due to the low melting point of MoO_3 (m.p. 795°C), this oxide being a major contamination of WO_3. The source of K is not clear at present. This evaporation modifies the melt composition during pulling leading to thermal melt instability, non-flat liquid–solid interface, non-uniform crystal diameter and a non-uniform Nd incorporation. The sintering procedure described above improves these aspects and further purification of the starting compounds is expected to improve the final results. Nevertheless it is worth noting that possible Mo or K contamination of the NBW studied crystal is well below the analytical sensitivity and therefore does not influence the spectroscopy of Nd. Further details of the crystal growth procedure as well as of characterization of the sample can be found elsewhere [9].

Nd doped NBW crystals with dimensions of several centimetres were grown using Pt crucibles with pulling rates in the 0.8–4 mm/h range and crystal rotation rates between 6 and 10 rpm. The melting temperature was 935°C. Nd concentrations in the crystal up to $[Nd] = 0.3 \times 10^{20}$ cm^{-3} were achieved with good optical quality. With the procedure at present developed, above this Nd concentration crystal cracks, inclusions and even polycrystalline regions were observed.

4. Optical spectroscopy

Optical absorption (OA) was recorded in a Variant 5E spectrophotometer. Continuous wave photoluminescence (PL) was excited with the ultraviolet multiline emission of a 5 W Ar laser, the emission was analysed with a Spex 340E spectrometer and detected with a cooled R928 Hamamatsu photomultiplier, or a 77 K cooled Ge photodiode and a lock-in amplifier. For OA and PL experiments the samples were cooled to 10 K using a He close cycled cryostat connected to a suitable temperature controller.

Fig. 1 gives an overview of the 10 K polarised OA spectra for Nd^{3+}. From these measurements the energies of the Stark levels from $^4I_{13/2}$ up to $^2I_{11/2}$ have been determined. J-manifolds of $4f^3$ configuration of Nd^{3+} are split in $(J+1)/2$ Stark levels. The presence of a single band from the ground level to the $^2P_{1/2}$ multiplet would suggest the existence of a unique site for Nd^{3+} in the crystal. This would agree with the assumption of the centrosymmetric crystal structure and, therefore, with a C_2 site symmetry for Nd^{3+}, but from this symmetry no polarisation rules are expected for the Nd^{3+} intraionic transitions, in contrast with the results shown in Fig. 1.

It must be noted, however, that the spectral widths of the absorption lines of Nd^{3+} in NBW are in most cases larger than in other crystalline hosts. For instance, the $^4I_{9/2} \rightarrow {}^2P_{1/2}$ transition in NBW has a bandwidth of 21 cm^{-1} while in most crystals it is ≈8–10 cm^{-1}. The widths of some OA bands, which do not appear strongly overlapped, are included in Table 1. The large band-width could be due to the overlapping of the OA of several centres, therefore, the contribution of the two centres assumed for the non-centrosymmetric crystal structure must be examined. For this purpose in what follows we have made a crystal field (cf) analysis of the Nd^{3+} energy levels in NBW.

Energy level positions of the ground $^4I_{9/2}$ and first excited $^4I_{11/2}$ multiplets have been established from the PL lowest $^4F_{3/2}$ level shown in Fig. 2. Lesser intensity emission bands arising from the $^4F_{3/2}$ high-energy component, 62 cm^{-1} above, unambiguously reproduce the sequence of these $^4I_{9/2}$ and $^4I_{11/2}$ crystal field levels (Fig. 2). From the OA and PL experiments, the energies of the 90 levels summarised in Table 1 have been determined. For the cf calculations we have excluded the five $^2H_{11/2}$ levels, which are argued to be affected by a non-negligible mixing with some states of the $4f^25d^1$ excited configuration [10], and thus usually poorly reproduced by normal cf calculations.

5. Simulation of the cf energy levels and discussion

The energy of Nd^{3+} levels in solids can be properly simulated supposing the central field approximation which considers separate Hamiltonians for free ion (fi) and crystal field (cf) interactions. The effective free ion Hamiltonian H_{FI} used here for Nd^{3+} includes up to 20 fi parameters [11]. The one-electron crystal field potential H_{CF} is expressed as a sum of products of tensor operators $(C_q^k)_i$, with real B_q^k and complex S_q^k parameters as coefficients [12]:

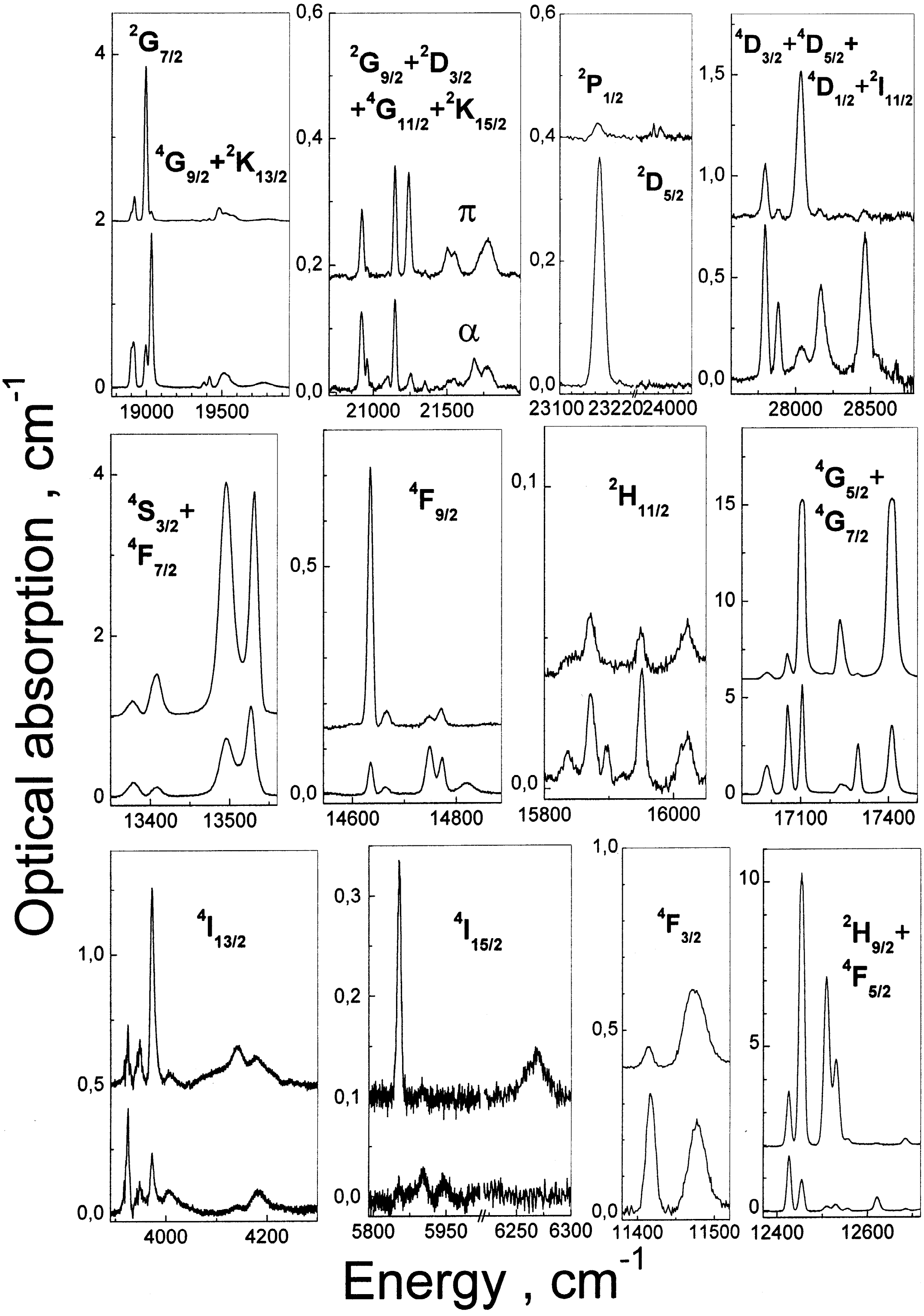

Fig. 1. Polarised 10 K optical absorption of Nd^{3+} in $NaBi(WO_4)_2$ single crystal $[Nd]=0.3\times10^{20}$ cm^{-3}. α spectra (E⊥c, H⊥c); π spectra (E//c, H⊥c).

$$H_{CF}=\sum_{k=2}^{4,6}\sum_{q=0}^{k}\left[B_q^k(C_q^k+(-1)^qC_{-q}^k)+iS_q^k(C_q^k-(-1)^qC_{-q}^k)\right] \qquad (1)$$

where the values of k and q for which the parameters are non-zero depend on the considered site symmetry.

When the S_4 symmetry is considered for Nd^{3+} in NBW, the cf potential involves five real B_q^k and two complex S_q^k

Table 1
10 K observed (E_o) and calculated (E_c) energy levels (cm^{-1}) of Nd^{3+} in NaBi(WO$_4$)$_2$ crystals in a single site of C$_2$ symmetry and for two possible S$_4$ symmetry sites. ΔE is the experimental OA line-width

$^{2S+1}L_J$	E_o (ΔE)	E_c-C$_2$	E_c1-S$_4$	E_c2-S$_4$
$^4I_{9/2}$	0	11	0	0
	104	104	120	156
	156	156	221	157
	228	234	330	257
	435	438	544	561
$^4I_{11/2}$	1961	1960	1998	2005
	1997	1992	2064	2040
	2014	2014	2072	2042
	2042	2052	2113	2069
	2161	2172	2244	2247
	2178	2194	2286	2274
$^4I_{13/2}$	3924 (8)	3918	3944	3951
	3948 (12)	3937	4001	3977
	3970 (10)	3970	4015	3990
	4008 (29)	3993	4070	4017
	4142 (26)	4142	4238	4234
	–	4171	4257	4249
	4182 (30)	4181	4258	4251
$^4I_{15/2}$	5853 (9)	5859	5827	5839
	5903 (13)	5899	5923	5920
	5945 (19)	5956	5991	5931
	–	5988	6094	6027
	6234	6227	6314	6322
	6271 (24)	6259	6355	6373
	–	6305	6453	6419
	6340	6341	6490	6481
$^4F_{3/2}$	11415 (16)	11402	11450	11466
	11477 (31)	11454	11533	11495
$^4F_{5/2}$ and $^2H_{9/2}$	12426 (11)	12412	12461	12467
	12454 (15)	12449	12507	12486
	12509 (16)	12509	12541	12510
	12529 (16)	12546	12585	12590
	12555	12554	12614	12604
	12620 (13)	12627	12701	12683
	12684 (14)	12660	12737	12722
	12716	12714	12821	12790
$^4F_{7/2}$	13378 (17)	13385	13411	13438
	13408 (16)	13420	13477	13451
$^4S_{3/2}$	13496 (20)	13494	13568	13554
	–	13501	13579	13557
$^4F_{7/2}$	13526	13521	13594	13584
	13531 (14)	13524	13632	13596
$^4F_{9/2}$	14635 (13)	14650	14713	14712
	14664 (17)	14677	14743	14729
	14749 (17)	14748	14818	14808
	14773 (10)	14781	14822	14827
	14821 (29)	14832	14919	14870
$^2H_{11/2}$	15835 (15)	15898	15949	15932
	15872 (15)	15906	15951	15940
	15896 (9)	15918	15976	15955
	15951 (11)	15933	15997	15972
	–	15949	16011	16004
	16021 (22)	15975	16058	16032
$^4G_{5/2}$	16987 (29)	16981	17070	17020
	17053 (20)	17036	17104	17095
	17105 (23)	17104	17166	17144
$^4G_{7/2}$ (*$^2G_{7/2}$)	17233	17233	17302	17282
	17253	17240	17307	17304
	17294 (18)	17294	17383	17352
	17411 (36)	17421	17509	17498
$^2G_{7/2}$ (*$^4G_{7/2}$)	18899 (20)	18893	18951	18926
	18912 (20)	18926	18977	18979
	18994 (26)	19011	19101	19076
	19030 (25)	19044	19124	19081
$^4G_{9/2}$	–	19323	19375	19344
	19379	19384	19440	19427
	19417	19418	19482	19463
$^2K_{13/2}$	19479	19476	19524	19554
	19512	19494	19539	19571
	19521	19522	19583	19573
$^4G_{9/2}$	19540	19530	19598	19599
$^2K_{13/2}$	–	19564	19627	19602
	–	19600	19672	19621
	–	19623	19679	19718
	19777	19776	19925	19846
	–	19852	19931	19862
$^2G_{9/2}$	20923	20936	20983	20967
	20958	20963	21024	21016
	–	20980	21044	21035
	–	21000	21052	21038
	21085	21076	21119	21110
$^2D_{3/2}$	21095	21095	21166	21138
	21146	21118	21181	21141
$^4G_{11/2}$ and $^2K_{15/2}$	21239	21242	21306	21269
	21257	21259	21341	21320
	21350	21347	21446	21401
	21503	21495	21487	21574
	–	21519	21545	21588
	21543	21550	21597	21633
	–	21571	21643	21634
	–	21595	21671	21664
	–	21606	21704	21700
	–	21651	21737	21701
	–	21679	21769	21725
	21687	21686	21778	21754
	21772	21766	21901	21836
	–	21833	21930	21862
$^2P_{1/2}$	23179 (21)	23186	23252	23241
$^2D_{5/2}$	23683	23690	23735	23778
	23739	23749	23807	23802
	23821	23814	23937	23851
$^2P_{3/2}$	–	26117	26161	26183
	–	26181	26264	26217
$^4D_{3/2}$	–	27678	27704	27751
	27794 (40)	27792	27835	27849
$^4D_{5/2}$	27883 (41)	27919	28240	27952
	28037 (65)	28053	28050	28150
	28166 (72)	28148	28098	28162
$^4D_{1/2}$	28462 (68)	28430	28531	28475
$^2I_{11/2}$	28960	28960	28964	29039
	29043	29037	29143	29094
	29124	29143	29213	29176
	–	29251	29252	29301
	–	29392	29453	29432
	–	29431	29492	29452

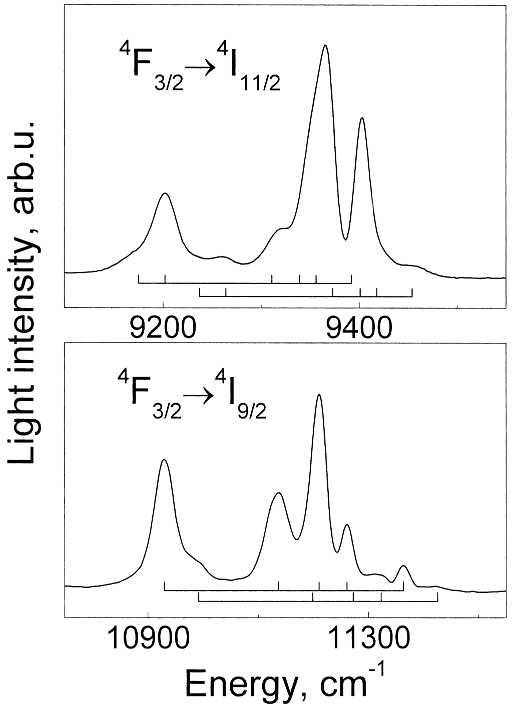

Fig. 2. $^4F_{3/2}$ non-polarised 10 K photoluminescence of Nd^{3+} in $NaBi(WO_4)_2$ single crystal. The bars show the contributions of the upper and lower Stark $^4F_{3/2}$ levels.

parameters, however, if the site symmetry is supposed to be C_2 the number increases to nine real and six complex parameters. In both situations one complex cf parameter, S_4^4 or S_2^2, respectively, is cancelled by an appropriate choice of the reference axis system.

We have used the very simplified simple overlap model (SOM) [13] to provide starting cf parameters as

$$B_q^k = \langle r^k \rangle \sum_{\mu} \rho_{\mu} \left(\frac{2}{1 \pm \rho_{\mu}} \right)^{k+1} A_q^k(\mu), \quad \rho_{\mu} = \rho_0 \left(\frac{R_0}{R_{\mu}} \right)^{3.5} \qquad (2)$$

Detailed description of the above expressions can be found elsewhere [13]. The advantage of SOM in comparison to other empirical models lies in the consideration of only the first neighbours of R, with the values of the effective charge for the oxygen and the overlap ρ between orbitals of R and oxygen as the two unique adjustable parameters. The symmetry properties of the Nd^{3+} site and the effective charge attributed to ligands are taken into account through the charge lattice sums, A_q^k, and the radial integrals $\langle r^k \rangle$ for Nd^{3+}. ρ varies for each ligand as a function of the distance, R_{μ}, according to the indicated potential law, R_o being the shortest distance.

Nd^{3+} is expected to replace Bi^{3+} in the NBW host. In order to minimise the simulation uncertainty we started with Nd^{3+} fi parameters determined in $Na_5Nd(MoO_4)_4$ having a similar site symmetry [14], some of them fixed to standard values [11]. Initial cf parameters calculated from SOM assume Nd^{3+} in the crystallographic position of Bi1 or Bi2, both with S_4 symmetry, and the respective neighbours given in Ref. [6]. After convergence of each one of separated fits of the whole observed energy level scheme given in Table 1, the assumption of Nd^{3+} in a Bi2 site provides the lowest root mean square deviation, σ (see Table 2 footnote for definition). The best collection of five real B_q^k and one complex S_q^k cf and fi refined parameters was selected then as the starting set in the calculation performed applying the descent of symmetry method assuming a C_2 site symmetry for Nd^{3+} in NBW. The

Table 2
Free ion and cf parameters (cm^{-1}) for Nd^{3+} in $NaBi(WO_4)_2$ crystals[a]

	C_2	1-S_4 (2*b*)	2-S_4 (2*c*)
E^0	23484 (1)	23553(1)	23537(1)
E^1	4792 (7)	4792 (7)	4792 (7)
E^2	23.15 (2)	23.15 (2)	23.15 (2)
E^3	479.98 (8)	479.98 (8)	479.98 (8)
α	21.90 (2)	21.90 (2)	21.90 (2)
β	−686 (3)	−686 (3)	−686 (3)
γ	[1500]	[1500]	[1500]
ζ	890.4 (6)	890.4 (6)	890.4 (6)
M^0[b]	2.05 (6)	2.05 (6)	2.05 (6)
P^2[c]	27.75 (13)	27.75 (13)	27.75 (13)
T^2	[348]	[348]	[348]
T^3	30 (2)	30 (2)	30 (2)
T^4	93 (2)	93 (2)	93 (2)
T^6	−283 (5)	−283 (5)	−283 (5)
T^7	326 (6)	326 (6)	326 (6)
T^8	[331]	[331]	[331]
B_0^2	386 (18)	707	278
B_2^2	100 (14)	–	–
B_0^4	−1011 (33)	−942	−975
B_2^4	229 (42)	–	–
S_2^4	−90 (59)	–	–
B_4^4	−664 (33)	951	1100
S_4^4	−795 (26)	−305	79
B_0^6	−96 (46)	–	–
B_2^6	−63 (39)	–	–
S_2^6	−179 (63)	–	–
B_4^6	−717 (23)	1141	1177
S_4^6	−363 (32)	−254	−243
B_6^6	−68 (45)	–	–
S_6^6	−98 (44)	–	–
S_2	184	316	125
S_4	605	547	612
S_6	328	466	472
S_T[d]	411	454	452
l Stark levels	85		
σ[e]	13.6		
Residue	10775.6		

[a] Values in parentheses refer to e.s.d. in the indicated parameter. Values in square brackets were not allowed to vary in the parameter fitting. All data are in cm^{-1} units.

[b] M^0, M^2, M^4 were constrained by the ratios $M^2 = 0.5625\ M^0$, $M^4 = 0.3125\ M^0$.

[c] P^2, P^4, P^6 were constrained by the ratios $P^4 = 0.75\ P^2$, $P^6 = 0.50\ P^2$.

[d] $S_k = \{1/(2k+1)[(B_0^k)^2 + 2\Sigma_q[(B_q^k)^2 + (S_q^k)^2]]\}^{1/2} S_T = \left[\frac{1}{3} \Sigma_k S_k^2 \right]^{1/2}$.

[e] $\sigma = [\Sigma(\Delta_i)^2/(l-p)]^{1/2}$, $\Delta = E_o - E_c$, l, number of levels, p number of parameters.

simulation yielded an energy level sequence in accordance with observed data, for which a very low $\sigma = 13.6$ cm^{-1} value was obtained. Final results of this adjustment are summarised Table 1, energy levels, and Table 2, fi and cf parameters.

To account for the influence of the two possible sites in S_4 symmetry, we have used the optimised fi parameters of Table 1 together with the cf parameters deduced by the SOM with either the Bi1–O or Bi2–O distances of Ref. [6]. Level energy sequences derived for both sites are also given in Table 1. In both cases, the ground levels have been adjusted to 0 cm^{-1} through the displacement of E^0. The energy differences between equivalent levels for both S_4 sites are generally similar to the line-width of the corresponding experimental OA band. It is therefore likely that these two different sites were not resolved in the experimental OA and PL measurements.

Table 2 also includes SOM calculated sets of cf parameters corresponding to both S_4 optical centres. Calculated total crystal field strengths S_T, a way to compare cf effects, especially when the number of involved cf parameters is large, are very similar in all cases, and for the two S_4 centres they have almost the same values. The closeness between S_2 values, which are very sensitive to the magnitude of the electrostatic interactions, i.e. to the Nd–oxygen distances, for C_2 and 2-S_4 simulations, supports the reliability of the used starting set of cf parameters.

However, the simple assumption of two Nd^{3+} centres with S_4 site symmetry and both having parallel principal symmetry axes (expected from the crystallographic model) is inconsistent with the polarisation features observed in OA spectra. For instance, if we assume that the $^4I_{9/2} \rightarrow {}^2P_{1/2}$ transition is only seen in an α spectrum, the $^4I_{9/2} \rightarrow {}^4S_{3/2} + {}^4F_{7/2}$ transitions should exhibit three α bands that are not allowed in the π spectrum, this being inconsistent with the experimental result of Fig. 1. This disagreement between experimental results and group theory selection rules is not due to an inaccuracy in the orientation of the crystal. In fact, this problem has been already noticed in the assigning of Raman and IR vibration modes of the NBW host [6].

To explain these results together with the enlargement of experimental line-widths, two possibilities should be considered in the light of the crystal field theory. Either the symmetry of the single Nd^{3+} site in NBW is lower than S_4, i.e. C_2 [5], with no selection rules expected for OA, or following previous suggestions [6], short-range order and non-random distribution are affecting the Na^+ and Bi^{3+} environments of Nd^{3+} in NBW. In the latter case, each one of the two optically active Nd^{3+} sites in S_4 symmetry would be inhomogeneously broadened and perhaps with different principal optical axis due to the influence of the Na and Bi short-range environment. To obtain more experimental evidence of the coexistence of the two possible Nd substituted centres, time-resolved spectroscopy and radiative lifetime measurements are currently in progress.

6. Conclusions

Nd doped $NaBi(WO_4)_2$ crystals can be successfully grown by the Czochralski technique with a Nd concentration in the crystal up to 0.3×10^{20} cm^{-3}. The energies of 90 Nd^{3+} Stark levels have been experimentally determined and the influence of the polarisation of the light on the optical absorption has been evidenced. According to the crystallographic models at present available for NBW, the consequences on the OA of the assumption of a single Nd^{3+} centre with C_2 symmetry, or two centres in S_4 site symmetry have been discussed. The latter assumption is consistent with the experimental OA line-widths but further changes in the site symmetry should be assumed to account for the polarisation rules observed. The adjustment of observed crystal field levels has provide a good set of fi and cf parameters for Nd^{3+} in NBW.

Acknowledgements

This work is supported by CICyT under grant numbers 2FD97-0912 and MAT1999-1077. A.M. is supported by CONACYT (Mexico). V.V. acknowledges support by a sabbatical grant SAB-1995-0709 of the Spanish Education Ministry.

References

[1] V.K. Tzunov, V.A. Efremov, Yu.A. Velihkodnyi, Crystallochemistry and Properties of Double Molybdates and Tungstates, Nauka, Leningrad, 1986.

[2] A.A. Kaminskii, H.J. Eichler, K. Ueda, N.V. Klassen, B.S. Redkin, L.E. Li, J. Findeisen, D. Jaque, J. García-Solé, J. Fernández, R. Balda, Appl. Opt. 38 (1999) 4533.

[3] K. Nitsch, M. Nikl, C. Barta, D. Schultze, A. Triska, R. Uecker, Phys. Status Solidi (a) 118 (1990) K133.

[4] A.A. Kaminskii, S.N. Bagayev, K. Ueda, H. Nishioka, Y. Kubota, X. Chen, A. Kholov, Jpn. J. Appl. Phys. 34 (1995) L1461.

[5] J. Hanuza, M. Maczka, J.H. van der Maas, J. Solid State Chem. 117 (1995) 177.

[6] J. Hanuza, A. Benzar, A. Haznar, M. Maczka, A. Pietraszko, J. H van der Maas, Vib. Spec. 12 (1996) 25.

[7] V. Volkov, C. Zaldo, J. Cryst. Growth 206 (1999) 60.

[8] P.V. Klevtsov, V.A. Vinokurov, R.F. Klevtsova, Kristallografiya 18 (1973) 1192.

[9] V. Volkov, M. Rico, A. Méndez-Blas, C. Zaldo, J. Phys. Chem. Solids (in press).

[10] D. Garcia, M. Faucher, J. Chem. Phys. 90 (1989) 5280.

[11] W.T. Carnall, G.L. Goodman, K. Rajnak, R.S. Rana, J. Chem. Phys. 90 (1989) 3443.

[12] B.G. Wybourne, Spectroscopic Properties of Rare Earth, Wiley, New York, 1965.

[13] P. Porcher, M. Couto dos Santos, O. Malta, Phys. Chem. Chem. Phys. 1 (1999) 397.

[14] E. Antic Fidancev, C. Cascales, M. Lemaitre Blaise, P. Porcher, J. Alloys Comp. 207/208 (1994) 178.